

Urban Aerosols and Their Interaction with Clouds and Rainfall: A Case Study for New York and Houston

MENGLIN JIN,¹ J. MARSHALL SHEPHERD,² AND MICHAEL D. KING³

Short title: Urban Aerosols and their Interaction with Clouds and Rainfall

Journal of Geophysical Research
(Manuscript submitted June 1, 2004)

¹ Department of Meteorology, University of Maryland, College Park, Maryland.

² Laboratory for Atmospheres, NASA Goddard Space Flight Center, Greenbelt, Maryland.

³ Earth Sciences Directorate, NASA Goddard Space Flight Center, Greenbelt, Maryland.

Authors - Dr. Menglin Jin
Department of Meteorology
University of Maryland
College Park, MD 20742
(301) 405-8833
(301) 314-9482 (fax)
mjin@atmos.umd.edu

Dr. J. Marshall Shepherd
NASA Goddard Space Flight Center
Code 912
Greenbelt, MD 20771
(301) 614-6327

Dr. Michael D. King
NASA Goddard Space Flight Center
Code 900
Greenbelt, MD 20771
(301) 614-5636

Abstract

Diurnal, seasonal, and interannual variations of urban aerosols were analyzed using 4-years of NASA Earth Observing System (EOS) Moderate Resolution Imaging Spectroradiometer (MODIS) observations, *in situ* AErosol RObotic NETwork (AERONET) observations, and *in situ* EPA PM_{2.5} data for one mid-latitude city (New York) and one sub-tropical city (Houston). Seasonality is evident in aerosol optical thickness measurements, with a minimum in January and a maximum in April to July. The diurnal variations of aerosols, however, are largely determined by local and regional weather conditions, such as surface and upper-level winds. On calm clear days, aerosols peak during the two rush hours in the morning and evening. In addition, corresponding cloud properties observed from MODIS and rainfall measurements from NASA's Tropical Rainfall Measuring Mission (TRMM) demonstrate an opposite phase to the seasonality of aerosols. Furthermore, the human-activity-induced weekly cycle of aerosols and clouds are detectable, but are weak as the human-activity signal is mixed with noises of natural weather systems. These analyses suggest typical spatial and temporal variations that illustrate the linkages and feedbacks between the urban environment, water cycle processes, and climate.

1. Introduction

Aerosol-cloud interaction is one of the weakest parts in current climate modeling [Randall, personal communication, 2002]. Better quantitative understanding of the spatial and temporal aerosol properties is desired in order to include aerosol radiative forcing and aerosol-cloud interactions in a general circulation model (GCM). Furthermore, observed climatological relationships between aerosols, clouds, and rainfall are needed for validating the modeled aerosol-cloud-rainfall interactions in urban areas. This paper aims to describe the temporal variations of aerosol and to identify monthly mean aerosol-cloud-rainfall relationships from various remote sensing and ground-based measurements. Specifically, diurnal, weekly, seasonal, and interannual variations of urban aerosols are studied using 4-years of aerosol, cloud, rainfall, and land cover (namely, normalized difference vegetation index, NDVI) measurements from NASA satellites. We emphasize on one mid-latitude city (New York) and one sub-tropical city (Houston) to demonstrate the similarities and differences of urban aerosol in different climate regions. In addition, the surface pressure and wind from NCEP reanalysis are used to examine how atmospheric system control the transport of urban aerosols.

Aerosol radiative forcing, the so-called “direct effect,” means that aerosols reduce surface insolation by scattering and absorbing solar radiation and reemitting longwave radiation back to the surface [Ramanathan *et al.*, 2001]. In addition, aerosols affect the climate system through aerosol-cloud interactions, primarily in three ways: (i) aerosols reduce the cloud effective radius and increase the cloud optical thickness as cloud condensation nuclei (CCN) increase, viz., the “indirect effect” [Twomey, 1977; King *et al.*, 1993]; (ii) aerosol heating changes atmosphere stability and thus the occurrence and evaporation of clouds (“semi-

indirect effect”) [*Hansen et al.*, 1997]; and (iii) clouds affect aerosol properties. For example, it was reported that the cloud diurnal cycle affects aerosol forcing over the Indian Ocean Experiment up to $1\text{--}2\text{ Wm}^{-2}$ (*Podgomy et al.* [2001], manuscript unpublished). Similarly, aerosol size distribution can be changed due to aerosol-cloud interactions [*Remer and Kaufman*, 1998].

Produced by combustion of fossil fuels from traffic or industrial processes and modified through chemical composition, decomposition, and transport, urban aerosols are directly related to human life and are gaining increasing attention [*IPCC*, 2001; *Lelieveld et al.*, 2001; *Ramanathan et al.*, 2001; *Kaufman et al.*, 2002]. Figure 1 shows the simulated aerosol-induced changes in surface insolation based on the AERONET-observed aerosol optical properties for New York on one day in September (September 1, 2001). The total reduction in insolation for this day is about 20 Wm^{-2} , with the maximum reduction at $0.55\text{ }\mu\text{m}$ between clean and polluted cases. The calculation uses the NASA Global Modeling and Assimilation Office’s (GMAO’s) GCM radiative transfer scheme [*Chou and Suarez*, 1999]. The model requires input of aerosol optical thickness, single scattering albedo, asymmetry factor, vertical aerosol distribution, and cloud cover. Clearly, to study aerosol impacts, these spatial and temporal properties of urban aerosols are required.

Spectral aerosol optical thickness is the key parameter for modeling the radiative effects of aerosols in atmosphere columns, and is well determined by the MODIS remote sensing algorithm [*Kaufman et al.* 1997; *Chu et al.*, 2002, 2003]. Therefore, we study optical thickness to represent the interactions between aerosols and clouds. Furthermore, urban aerosol enhances aerosol-cloud interaction, which is expected to be more significant during the summer months when large-scale dynamic impact is relatively weak than in winter.

Scale is critical in urban studies, as urban features vary dramatically along

both horizontal and temporal dimensions [Oke, 1982; Jin *et al.*, 2004]. We analyzed cloud-rainfall-aerosol relationships at monthly instead of daily scale, in particular, because we intended to identify the typical, climatological sense of aerosol properties and their effects on clouds and rainfall, and partly because the daily variations are more affected by white noise from surface and atmospheric conditions than the longer scales, and thus are not the major focus of this study.

The second section describes the data sets used in this work. The third section presents the results, and is followed by social, land cover, and general circulation backgrounds for New York and Houston that may shed light on explaining the differences in the aerosol properties for these two cities. Final remarks are presented in Section 5.

2. Data Sets

MODIS Aerosol and Cloud Products – Terra/MODIS monitors the aerosol optical thickness over the globe from a 705 km polar-orbiting sun-synchronous orbit that descends from north to south, crossing the equator at 10:30 local time. The aerosol optical thickness (τ_a) over land is retrieved at 0.47, 0.56 and 0.65 μm and at a 10 km spatial resolution using the algorithm described by Kaufman *et al.* [1997]. The spectral dependence of the reflectance across the visible wavelengths is then used to obtain a rough estimate of the fine mode (radius < 0.6 μm) fraction of the aerosol optical thickness at 0.56 μm . The cloud optical thickness (τ_c) and effective radius (r_e) are retrieved at 1 km spatial resolution using the algorithm described by King *et al.* [1992] and Platnick *et al.* [2003]. These variables, as well as all other atmospheric properties from MODIS, are aggregated at daily, eight-day, and monthly time intervals on a global $1^\circ \times 1^\circ$ latitude-longitude grid. These Level-3 products contain simple statistics (mean, standard deviation, etc.) computed for each parameter, and also contain marginal density and joint prob-

ability density functions between selected parameters [King *et al.*, 2003].

MODIS aerosol and cloud properties have been validated by through field experiments and intercomparisons with ground-based observations [Chu *et al.*, 2002; Mace *et al.*, 2004]. Monthly mean aerosol and cloud products from Terra between April 2000 and September 2003 are utilized in the present study. In addition, daily cloud products from June to September 2001 are used for analysis of the weekly cycle of summer time urban aerosols.

EPA PM_{2.5} data – Because Terra/MODIS only provides daytime measurements of aerosol optical thickness at ~10:30 AM local time for clear conditions, *in situ* EPA PM_{2.5} measurements are used to monitor the diurnal variation of aerosol concentration in this work. PM_{2.5} refers to particle mass of particles less than 2.5 μm diameter that generally consists of mixed solid and liquid aerosols in air and which excludes dust. PM_{2.5} therefore captures the “fine” mode particles that are $\leq 2.5 \mu\text{m}$ in diameter.

AERONET daily data – AErosol RObotic NETwork (AERONET) provides ground-based aerosol monitoring and data archive at ~170 locations worldwide. Data of spectral aerosol optical thickness, size distribution, single scattering albedo, and precipitable water in diverse aerosol regions provide globally-distributed near real time observations of aerosols [Holben *et al.*, 1998]. Hourly and daily AERONET measurements of aerosol optical thickness are used to identify the diurnal and weekly cycles of aerosol. The data are quality-ensured and cloud-screened [Eck *et al.*, 1999; Smirnov *et al.*, 2000].

TRMM Rainfall Data – TRMM was launched in November 1997 as a joint U.S.-Japanese mission to advance the understanding of the global energy and water cycle by providing distributions of rainfall and latent heating over the global tropics [Simpson *et al.*, 1988; Shepherd *et al.*, 2002]. To extend TRMM data from 40°N-40°S, we use the 3B42 monthly, 1° x 1° rain rate and rain accumulation

product (Adler et al. 2000). . This product uses TRMM microwave imager data to adjust merged infrared precipitation and root-mean-square precipitation error estimates. It should be noted that the quality of Product 3B-42 is highly sensitive to the quality of the input infrared and microwave data. If the quality of the input data sources is less than anticipated, then the quality of product 3B-42 will be degraded. Nevertheless, these corresponding, multi-year rainfall products help establish the relationships between aerosols, clouds, and precipitation.

NDVI data – A 20-year NDVI data set derived from AVHRR channel 1 and channel 2 radiances is used to compare the vegetation/land cover changes in the New York and Houston regions. This data set is at 8 km and produced at a monthly resolution.

NCEP reanalysis – The National Centers for Environmental Prediction (NCEP) Reanalysis and National Center for Atmospheric Research (NCAR) 50-year reanalysis [Kistler et al., 2001] is used to reproduce the surface temperature and surface wind. The monthly-averaged model output has a spatial resolution of $2.5^{\circ} \times 2.5^{\circ}$. The NCEP reanalysis, like any other GCM output, has uncertainties, but the overall geographical distribution is proven to be realistic, and therefore suitable for use in providing weather conditions for New York and Houston.

3. Results

Figure 2 shows the global distribution of aerosol optical thickness at $0.56 \mu\text{m}$ over both land and ocean for June 2002, except for locations where the surface is too bright to be able to retrieve the aerosol loading (e.g., Sahara, Saudi Arabia, Greenland). These results are based on the monthly mean Terra/MODIS measurements for June 2002. Urban regions of North America, Europe, India, and East Asia have larger aerosol optical thicknesses than most of the inner continents, with the exception of biomass burning in Gabon and the Democratic Re-

public of the Congo, and dust outbreaks from the Sahara that is transported across the Atlantic. The radiative forcing of aerosols is generally larger over urban areas than the inner continents where urban aerosols are largely absent. The maximum $\tau_a \sim 0.8$ occurs along the Ganges Valley of India, large portions of China, and the eastern USA. It should be emphasized that τ_a arises from all types of aerosols, not just those of anthropogenic origins from urban areas alone.

Spatial values of τ_a ($0.56 \mu\text{m}$) change 10% for the New York region in three continuous summers, with above 0.5 in June 2000 and June 2002, but only around 0.4 in June 2001 (cf. Figure 3). Considering the change is on monthly mean scale, it is significant. In contrast, little change occurs in aerosol loading for three consecutive June months in Houston. Further study, as we will discuss below, suggests such differences are partly a result of local weather and climate conditions, and the subsequent transport of aerosols.

Aerosol loading at the surface in urban areas is typically the smallest at night and increases to the first maximum of the day at ~ 10 AM and then slightly drops in the afternoon until the arrival of the 2nd maximum of the day at about ~ 8 PM, as shown in Figure 4a. The peaks are likely caused by early morning and late afternoon car combustion resulting from the rush hours. However, on most days, the diurnal cycle is strongly modified by weather conditions and is thus less typical than the classic case illustrated in Figure 4a. Figure 4b shows that the peak aerosol quality index¹, occurs around 3 PM and afterwards, attains a value of only 0.20, which is half that of December 31, 2002. In addition, August 31,

¹ Air quality index is calculated by converting the measured pollutant concentrations into index values. To generate the index values, pollutant concentrations are expressed as a proportion of the Air NEPM standards or EPP (Air) goals, and then placed in a category based on that index value (see EPA web for details www.epa.qld.gov.au/environmental_management/air/air_quality_monitoring/air_quality_index)

2002 (Figure 4c) is even cleaner than September 11, 2002 (Figure 4b). Figure 4e shows the diurnal variation of aerosol index for Houston on December 31, 2002, and shows another pattern with small values during the daytime with a significant jump at night. Evidently, such jumps are due to transport of aerosols from outside the region.

Specific aerosol types may behave slightly differently from the total aerosol optical thickness. Low-level ozone in New York peaks in the late afternoon on August 22, 2002 (Figure 4d). By comparison, low-level ozone in Houston peaks at 10 AM, noon, and 3 PM on July 20, 2002 (Figure 4f).

Unlike variations at other longer time scales, the diurnal variation of aerosols is strongly controlled by local weather conditions, such as wind, which enhances the aerosol transport. Measurements from AERONET for the Goddard Institute locating in the New York City (Figure 5) show that on July 1, 2001, there was a sharp increase in spectral aerosol optical thickness, indicating aerosol transport from outside of the city. In fact, corresponding back-trajectory analyses of AERONET as well as NCEP surface wind data reveal the large aerosol transport from northern Canada. However, on calm, clear days such as July 2, 6, and 7, 2001 (Figures 5b, 5e, and 5f), the diurnal aerosol optical thickness is smooth and as low as 0.04. These three days are clear all day, and therefore AERONET is capable of providing long duration measurements. By contrast, aerosol optical thickness on July 3 and 5, 2001 was 0.06-0.08 in late morning and slightly increased in the late afternoon before the occurrence of clouds inhibited further measurements.

Pronounced seasonality with a minimum in winter and a maximum in April to early summer is observed in both New York City and Houston based on Terra/MODIS Level-3 data analysis for 3 years (cf. Figure 6). Minimum monthly mean aerosol optical thickness for Houston is <0.2 in the four continuous years

from 2000 to 2003, although the occurrence time of the minimum differs slightly: December in 2000, December to January in 2001, and November to January in 2002. The maxima are above 0.4 with the extreme value as high as 0.52 in April 2000. The maxima occur in April, corresponding to large-scale frontal or jet stream weather systems that typically occur during this transitional season. By contrast, the minimum τ_a ($0.56 \mu\text{m}$) in New York is 0.15, lower than that of Houston, and the maximum τ_a is above 0.5, consistent with that of Houston. In addition, New York's month-by-month variations are noisier than those of Houston. For example, January 2001 has a peak aerosol optical thickness while other Januarys have low optical thickness. NCEP reanalysis reveals that surface wind is much smaller in January 2001 than in other years (not shown), implying a weak aerosol transport responsible for the peak aerosol optical thickness in this month. This seems to indicate that urban aerosol concentration depends strongly on surface transport, determined by the surface-atmosphere circulation.

Given the warm anomalies over urban surfaces (i.e., urban heat island effect, *Jin et al.*, 2004), the urban atmospheric column would be less stable than the surrounding areas, indicating a higher probability of the city-induced convective activities [*Orville et al.*, 2001; *Shepherd et. al.* 2002, *Shepherd and Burian*, 2003]. The signal of human activities on the aerosol production can be seen from Figure 7a, which shows a weekly cycle of aerosol optical thickness over New York City as derived from AERONET observations, with the maximum occurring on weekdays and the minimum on weekends. These results are similar to those previously reported and have been hypothesized to be responsible for the weekly cycle of rainfall [*Cerveny and Balling*, 1998; *Linacre and Geerts*, 2002; *Marr and Harley* 2002a,b]. Correspondingly, a weekly cycle of cloud optical thickness is also evident (Figure 7b), with optically thicker clouds present on weekends than weekdays. A weekly cycle of cloud effective radius and integrated water path is

also observed (Figures 7c, 7d), where Figures 7a, 7b, and 7c are derived from daily Terra/MODIS level-2 cloud observations using the algorithm described by *Platnick et al.* [2003]. These weekly cycles are most likely a result of human activities since no natural forcing has a seven-day cycle in summer mid-latitudes.

Weekday-high aerosol optical thickness and weekend-high cloud properties are detectable for Houston, but relatively weak (cf. Figure 8). This is partly because the surface transport over Houston is generally stronger than in New York (cf. Figure 17), which distributes urban aerosols to other regions rapidly. In addition, the larger surface temperature in a sub-tropical city may induce stronger surface-layer and boundary layer mixing, which transports surface aerosols to the free atmosphere faster than mid-latitude cities.

Similarly, opposite relationships detected in weekly cycles between aerosol and cloud optical thickness can be observed from seasonal and interannual variations. Figure 9a shows variations of aerosol optical thickness, and Figure 9b shows the cloud optical thickness. In general, cloud optical thickness has minima during summers and maxima during winters, and ranges from 5-25. In addition, for water clouds, effective cloud droplet size has an opposite phase to cloud optical thickness. Namely, thick aerosol corresponds to high droplet size and low cloud optical thickness. It seems to be inconsistent with Twomey effect: when there are more aerosols, aerosols serve as CCN and reduce the size of cloud effective radius (cf. Figure 9b), and thus increases cloud optical thickness when the liquid water path of the atmosphere layer does not change [*Rosenfeld, 2000*]. However, part of Houston aerosol is transported from the sea (see Figure 17), and sea salt aerosols have large size and can increase cloud droplet size. Another reason is that we observe that more aerosols correspond to smaller ice cloud droplet size (not shown). This suggests that urban aerosols do reduce some water cloud droplets' size and these smaller droplets are easily uplifted to

higher altitudes to become ice cloud and thus reduce the averaged ice cloud droplets' size.

Urban-induced changes to clouds can be detected from the differences of clouds properties over urban and nearby non-urban regions. Figure 10 shows that in summer, clouds over the Houston region have smaller effective radii than clouds located east and south of Houston, and have larger effective radius than clouds located west and north of Houston. We focus on summer when mesoscale forcing is more dominant than large-scale, strongly forced events (e.g., frontal systems) over urban regions. Urban aerosols are part of the reason for the differences in cloud effective radius. Although the eastern, western, northern, and southern regions of Houston are only displaced 1° (~ 100 km) from the Houston region, the thermodynamic and kinetic conditions in the environment are quite different as shown from the monthly mean July surface pressure field (Figure 17). The surface wind is from south to north with high pressure centered to the east. This configuration transports urban aerosols to the northern and western regions, which may explain why these regions have smaller cloud effective radius than the regions to the east and south of Houston. Furthermore, Houston and surrounding regions all have consistent seasonality on cloud effective radius.

Seasonality of cloud top temperature for water clouds is similar to that of aerosol optical thickness, viz., low values in winter months and high values in summer months (Figure 11). This implies that a low aerosol optical thickness corresponds to cold water clouds and a high aerosol optical thickness corresponds to warm water clouds. A hypothesis is that if in Houston, large transport of sea salt aerosols makes column aerosol thickness high and increases cloud droplet size. The large cloud droplets can relatively hard to be uplifted to higher altitudes, and thus clouds have higher top temperatures.

Little seasonality is observed for rainfall over Houston and New York City suggesting that rainfall is less directly affected by aerosols than clouds (Figure 12). Around Houston, the TRMM-based accumulated rainfall data illustrated that the maxima monthly mean rainfall occurs in October 2000, May 2001, and September 2002, above 200 mm per month. This is consistent with the transition seasons in this region. In general, New York's rainfall has less month-to-month variation than Houston, with a maximum slightly above 200 mm/month in October 2002. Consequently, effective radius for water clouds is lower in New York City than in Houston (Figure 13a), implying a larger aerosol amount in New York City than in Houston's, which is consistent with results previously reported in Figures 3 and 6. It seems that with the increase of cloud effective radius for water clouds, accumulated rainfall increases. In contrast, Figure 13b is for ice clouds, which again show little relationship between effective radius and accumulated rainfall.

Analyzing monthly mean aerosol optical thickness vs. rainfall identifies little one-to-one relationship between aerosol and rainfall in a climatological sense. Figure 14 shows the increase of rainfall slightly corresponds to decrease of aerosol optical thickness. However, this is not detectable for New York City. *Shepherd and Burian* [2003] reported urban-induced rainfall anomalies in the downwind region of Houston. Understanding the mechanism responsible for rainfall anomalies is essential to simulating it in GCMs. The less direct relationship between rainfall and aerosol optical thickness as presented in Figure 14 implies that urban rainfall anomalies is not fully related to aerosol change. This observation is consistent with the recent hypothesis of *Shepherd and Burian* [2003] that dynamic processes like surface convergence and boundary destabilization are more dominant than aerosols for urban-induced convective events.

4. Background Conditions of New York and Houston

The urban aerosols and their effects vary from one city to another, depending on the city's microstructure (e.g., land use, building density, population density, and living styles), seasons, and prevailing environmental forcing [Oke, 1982; Karl *et al.*, 1988, Jin *et al.* 2004]. To understand aerosol and cloud differences between New York and Houston, some knowledge of the human population, land cover and land use, and large or regional scale weather systems for these two regions is essential.

Figure 15 is the human population during 1980-2000. New York City has a larger population, and consequently has more intense human activities and anthropogenic aerosol concentration. Specifically, New York has 12,558,314 people while Houston has only 4,465,671 (2000 census). This difference might contribute to factors causing New York to have higher τ_a than Houston in the summer months (Fig. 6).

Figure 16 shows the difference in the NDVI between July 1981 and July 2000. Both New York City and Houston have experienced significant land cover changes from 1980 to 2000, with corresponding changes in surface greenness. New York City and its surrounding region seem to have experienced a slightly larger NDVI change over the past 20 years as compared to Houston.

Figure 17 presents the monthly surface pressure field, which also indicates the surface wind speed and direction. Nevertheless, surface wind is also controlled by topography and thus may not exactly follow the pressure system. In July, Houston is close to a high pressure center that brings wind from the ocean. During this time period, Houston's surface circulation is dominated by more mesoscale circulations such as sea, bay, and heat island circulations, whereas New York's surface wind comes from the southeast (mostly land cover) and at a smaller speed than at Houston. This implies that Houston may have larger aero-

sol transport than New York, and ocean sea salt aerosol is transported into the city.

5. Final Remarks

Diurnal, seasonal, and interannual variations of aerosols have been studied using satellite, surface, and NCEP reanalysis data. This research reveals that spatial and temporal urban aerosols vary dynamically as a result of various parallel factors, such as human activity, land cover changes, cloud-aerosol interactions, and chemical processes. Therefore interdisciplinary knowledge, data, and expertise are needed to fully understand this topic.

Diurnal variations of aerosol are largely affected by weather conditions, but nighttime aerosol optical thickness is, in general, lower than that of daytime. Weekly variation of aerosol is a signal of human activity. In addition, seasonality of aerosol optical thickness has opposite phase with cloud optical depth and opposite phase with rainfall. Weekly cycles of urban aerosols and clouds, in particular, have been first observed in New York. This cycle may be interpreted as a signal of human activities. Nevertheless, this cycle may not be significant in other cities where aerosol transport is strong (like Houston), which implies this cycle is weaker than other temporal properties. By all means, the weekly cycle shows a possible human footprint on the local atmosphere-surface system, and is only statistically valid. Furthermore, As a result, aerosols reduce surface insolation. In a normal day of September, the aerosol-induced insolation is $20\text{--}30\text{ Wm}^{-2}$ (cf. Fig. 2).

Clearly, the dramatic increase and expansion of human activities in the past century has led to significant changes in land use and possible influences on the regional to global climate. Specifically, construction of new buildings and roads tends to disturb the natural land (and vegetation) morphology and enhance the

surface frictional effects on the atmospheric flows above. The resulting dynamical effects are to weaken surface flows but to increase the upward turbulent transport of aerosols.

The above results have important implications with respect to the modeling of aerosol-cloud interactions. Specifically, high-resolution satellite observations of aerosols, clouds, and rainfall could be used to update the atmospheric parameters for both numerical weather prediction and global (regional) climate models [Jin and Shepherd 2004]. The global distributions of aerosols and clouds could be utilized to initialize these models or validate the realisms of different model cloud microphysical processes.

Acknowledgments. We thank Brent Holben for the user-friendly on-line data archive and analysis system in support of AERONET. We also than Zhong Liu for developing an efficient on-line tool for MODIS, NDVI, and TRMM data. Special thanks go to Ming-Dah Chou for helpful discussions on his radiative transfer model. This work was funded by the NASA TRMM project under contract number PMM-0022-0069.

References

- Adler, R. F., G. J. Huffman, D. T. Bolvin, S. Curtis, and E. J. Nelkin, Tropical Rainfall distributions determined using TRMM combined with other satellite and rain gage information, *J. Appl. Meteor.*, 39(12), 2007-2023, 2000.
- Cerveny, R. S., and R. C. Balling, Jr., Weekly cycles of air pollutions, precipitation and tropical cyclones in the coastal NW Atlantic region, *Nature*, 394, 561-563, 1998.
- Chou, M. D., and M. J. Suarez, A solar radiation parameterization for atmospheric studies, NASA Tech. Memo 104606, Vol. 15, 40 pp., 1999.
- Chu, D. A., Y. J. Kaufman, C. Ichoku, L. A. Remer, D. Tanré, B. N. Holben, Vali-

- dation of MODIS aerosol optical depth retrieval over land, *Geophys. Res. Lett.*, 29(12), doi:10.1029/2001GL013205, 2002.
- Chu, D. A., Y. J. Kaufman, G. Zibordi, J. D. Chern, J. Mao, C. Li, and B. N. Holben, Global monitoring of air pollution over land from the Earth Observing System-Terra moderate resolution imaging spectroradiometer (MODIS). *J. of Geophys. Res.* 108(D21), 4461, doi:10.1029/2002JD003179, 2003.
- Eck, T. F., B. N. Holben, J. S. Reid, O. Dubovik, A. Smirnov, N. T. O'Neill, I. Slutsker, and S. Kinne, Wavelength dependence of the optical depth of biomass burning, urban, and desert dust aerosols, *J. Geophys. Res.*, 104(24), 31,333-31,349, 1999.
- Hansen J., M. Sato, and R. Ruedy, Radiative forcing and climate response, *J. Geophys. Res.*, 102, 6831-6864, 1997.
- Holben, B. N., T. F. Eck, I. Slutsker, D. Tanré, J. P. Buis, A. Setzer, E. Vermote, J. A. Reagan, Y. J. Kaufman, T. Nakajima, F. Lavenue, I. Jankowiak, and A. Smirnov, AERONET—A federated instrument network and data archive for aerosol characterization, *Remote Sens. Environ.*, 66, 1-16, 1998.
- IPCC, Intergovernmental Panel on Climate Change, *Climate Change 2001: The Scientific Basis. Contribution of working group 1 to the Third Assessment Report of the Intergovernmental Panel on Climate Change*, edited by J. T. Houghton et. al., 881 pp., Cambridge Univ. Press, New York, 2001.
- Jin, M., R. E. Dickinson, and D. Zhang, The footprint of urban climate change through MODIS, Submitted to *J. Climate*, 2004.
- Jin, M. and J. M. Shepherd, On including urban landscape in land surface model – How can satellite data help? Submitted to *Bull. AMS*, 2004.
- Karl, T. R., H. F. Diaz, and G. Kukla, Urbanization: Its detection and effect in the United States Climate Record, *J. Climate*, 1, 1099-1123, 1988.
- Kaufman, Y. J., D. Tanré, and O. Boucher, A satellite view of aerosols in the cli-

- mate system, *Nature*, 419, 215-223, 2002.
- Kaufman, Y. J., D. Tanré, L. A. Remer, E. F. Vermote, A. Chu, and B. N. Holben, Operational remote sensing of tropospheric aerosol over land from EOS Moderate Resolution Imaging Spectroradiometer, *J. Geophys. Res.*, 102, 17,051-17,067, 1997.
- King, M. D., Y. J. Kaufman, W. P. Menzel, and D. Tanré, Remote sensing of cloud, aerosol, and water vapor properties from the Moderate Resolution Imaging Spectrometer (MODIS), *IEEE. Trans. Geosci. Remote Sens.*, 30, 2-27, 1992.
- King, M. D., L. F. Radke, and P. V. Hobbs: Optical properties of marine stratocumulus clouds modified by ships, *J. Geophys. Res.*, 98, 2729-2739, 1993.
- King, M. D., W. P. Menzel, Y. J. Kaufman, D. Tanré, B. C. Gao, S. Platnick, S. A. Ackerman, L. A. Remer, R. Pincus, and P. A. Hubanks, Cloud and aerosol properties, precipitable water, and profiles of temperature and humidity from MODIS, *IEEE Trans. Geosci. Remote Sens.*, 41, 442-458, 2003.
- Kistler, R., E. Kalnay, W. Collins, S. Saha, G. White, J. Woollen, M. Chelliah, W. Ebisuzaki, M. Kanamitsu, V. Kousky, H. V. D. Dool, R. Jenne, and M. Fiorino, The NCEP-NCAR 50 year reanalysis: Monthly means CD-ROM and documentation, *Bull. Amer. Meteor. Soc.*, 82, 247-267, 2001.
- Lelieveld, J., P. J. Crutzen, V. Ramanathan, M. O. Andreae, C. A. M. Brenninkmeijer, T. Campos, G. R. Cass, R. R. Dickerson, H. Fischer, J. A. de Gouw, A. Hansel, A. Jefferson, D. Kley, A. T. J. de Laat, S. Lal, M. G. Lawrence, J. M. Lobert, O. L. Mayol-Bracero, A. P. Mitra, T. Novakov, S. J. Oltmans, K. A. Prather, T. Reiner, H. Rodhe, H. A. Scheeren, D. Sikka, and J. Williams, The Indian Ocean Experiment: Widespread air pollution from South and Southeast Asia, *Science*, 291, 1031-1036, 2001.
- Linacre, E., and B. Geerts, Estimating the annual mean screen temperature em-

- pirically, *Theor. Appl. Climat.*, 71, 43-61, 2002.
- Marr, L. C. and R. A. Harley, Spectral analysis of weekday-weekend differences in ambient ozone, nitrogen oxide, and non-methane hydrocarbon time series in California. *Atmos. Environ.*, 36, 2327-2335, 2002a.
- Marr, L. C., and R. A. Harley, Modeling the effect of weekday-weekend differences in motor vehicle emissions on photochemical air pollution in central California, *Environ. Sci. Technol.*, 36, 4099-4106, 2002b.
- Mace, G. G., Y. Zhang, S. Platnick, M. D. King, P. Minnis, and P. Yang: Evaluation of cirrus cloud properties derived from MODIS radiances using cloud properties derived from ground-based data collected at the ARM SGP site, *J. Appl. Meteor.*, in press, 2004.
- Oke, T. R., The energetic basis of the urban heat island, *Quart. J. Roy. Meteor. Soc.*, 108, 1-24, 1982.
- Platnick, S., M. D. King, S. A. Ackerman, W. P. Menzel, B. A. Baum, J. C. Riédi, and R. A. Frey, The MODIS cloud products: Algorithms and examples from Terra, *IEEE Trans. Geosci. Remote Sens.*, 41, 459-473, 2003.
- Ramanathan, V., P. J. Crutzen, J. T. Kiehl, and D. Rosenfeld, Aerosols, climate, and the hydrological cycle, *Science*, 294, 2119-2124, 2001.
- Remer, L. A., and Y. J. Kaufman, Dynamic aerosol model: Urban/industrial aerosol, *J. Geophys. Res.*, 103, 13859-13872, 1998.
- Rosenfeld, D., Suppression of rain and snow by urban and industrial air pollution, *Science*, 287, 1793-1796, 2000.
- Shepherd, J. M., and S. J. Burian, Detection of urban-induced rainfall anomalies in a major coastal city, *Earth Interactions*, 7(4), doi:10.1175/10873562(2003)007, 2003.
- Shepherd, J. M., H. Pierce, and A. J. Negri, Rainfall modification by major urban areas: Observations from spaceborne rain radar on the TRMM satellite, *J.*

Appl. Meteor., 41, 689-701, 2002.

Simpson, J., R. F. Adler, and G. R. North, A proposed Tropical Rainfall Measuring Mission (TRMM) satellite, *Bull. Amer. Meteor. Soc.*, 69, 278-295, 1988.

Smirnov, A., B. N. Holben, T. F. Eck, O. Dubovik, and I. Slutsker, Cloud screening and quality control algorithms for the AERONET data base, *Remote Sens. Environ.*, 73, 337-349, 2000.

Twomey, S., The influence of pollution on the shortwave albedo of clouds, *J. Atmos. Sci.*, 34, 1149-1152, 1977.

FIGURE LEGENDS

- Figure 1. Changes of surface solar radiation induced by urban aerosols for September 1, 2001, based on simulations from a radiative transfer model developed by *Chou and Suarez* [1999]. “diruv” and “difuv” represent direct and diffuse uv radiation, “dirpar” and “difpar” represent direct and diffuse photosynthetically active radiation, and “dirir” and “difir” represent direct and diffuse near-infrared radiation. The “total” represents the total solar radiation, and the values are shown on the right-hand axis in Wm^{-2} .
- Figure 2. Monthly average aerosol optical thickness at $0.56 \mu\text{m}$ for January 2002. These data are produced at a $1^\circ \times 1^\circ$ latitude-longitude grid worldwide, and are derived from Terra/MODIS measurements.
- Figure 3. Spatial distribution of aerosol optical thickness for the USA. Observations are from Terra/MODIS for (a) June 2000, (b) June 2001, and (c) June 2002.
- Figure 4. Diurnal variations of urban aerosols for New York and Houston on several days. Data are obtained from EPA PM_{2.5}. Aerosol index is the aerosol quality index. See text for details.
- Figure 5. Diurnal variation of aerosol optical thickness for New York City on several days of July 2001. Data are based on AERONET GISS station measurements.
- Figure 6. MODIS-derived monthly mean aerosol optical thickness at $0.56 \mu\text{m}$ from April 2000 to September 2003 for (a) Houston and (b) New York City.
- Figure 7. Weekly distribution of (a) the aerosol optical thickness from AERONET at the New York GISS station (41°N , 74°W); (b) the cloud optical thickness at $0.65 \mu\text{m}$ from the MODIS 1-km resolution level-2

data; (c) cloud effective radius; (d) cloud integrated water path. The data represent the median of the daily averages of June to September 2001 that are then spatially averaged over a 50 km x 50 km region centered on New York City.

Figure 8. MODIS-derived integrated water path as a function of the day of the week for Houston from July-September 2001.

Figure 9. MODIS-derived relationship between (a) aerosol optical thickness and (b) water cloud optical thickness (solid) and effective radius (dashed) for Houston.

Figure 10. MODIS-derived monthly mean cloud effective radius for Houston, and east, south, north, and south of Houston. Houston is located between 29° and 30°N, and 74° and 75°W.

Figure 11. Comparison of cloud top temperature of (a) Houston and (b) New York City derived from Terra/MODIS data.

Figure 12. TRMM observed monthly mean rainfall for (a) Houston and (b) New York City from January 2000 to September 2003. The observation product is 3B42, at 1° resolution.

Figure 13. Monthly mean accumulated rainfall vs. cloud effective radius for New York City and Houston (a) for water clouds and (b) for ice clouds.

Figure 14. The scatter plot of MODIS aerosol thickness and TRMM-based accumulated rainfall for Houston and New York City, respectively. The data are monthly mean values for the warm season period (June-September) for 2000, 2001, 2002, and 2003.

Figure 15. Population density of Houston and New York City from 1980 - 1999.

Figure 16. NDVI anomalies from 1981 to 2000 for (a) Houston and (b) New York City.

Figure 17. Monthly mean surface pressure for Houston (left) and New York City

(right) for July 2000. The data are from NCEP/NCAR reanalysis.

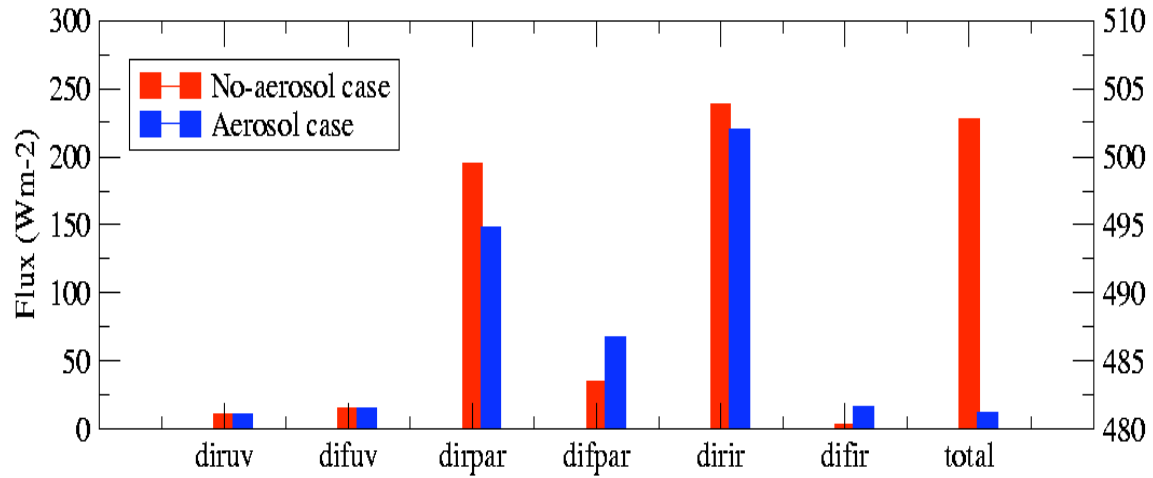


Figure 1. Changes of surface solar radiation induced by urban aerosols for September 1, 2001, based on simulations from a radiative transfer model developed by *Chou and Suarez* [1999]. “diruv” and “difuv” represent direct and diffuse UV radiation, “dirpar” and “difpar” represent direct and diffuse photosynthetically active radiation, and “dirir” and “difir” represent direct and diffuse near-infrared radiation. The “total” represents the total solar radiation, and the values are shown on the right-hand axis in Wm^{-2} .

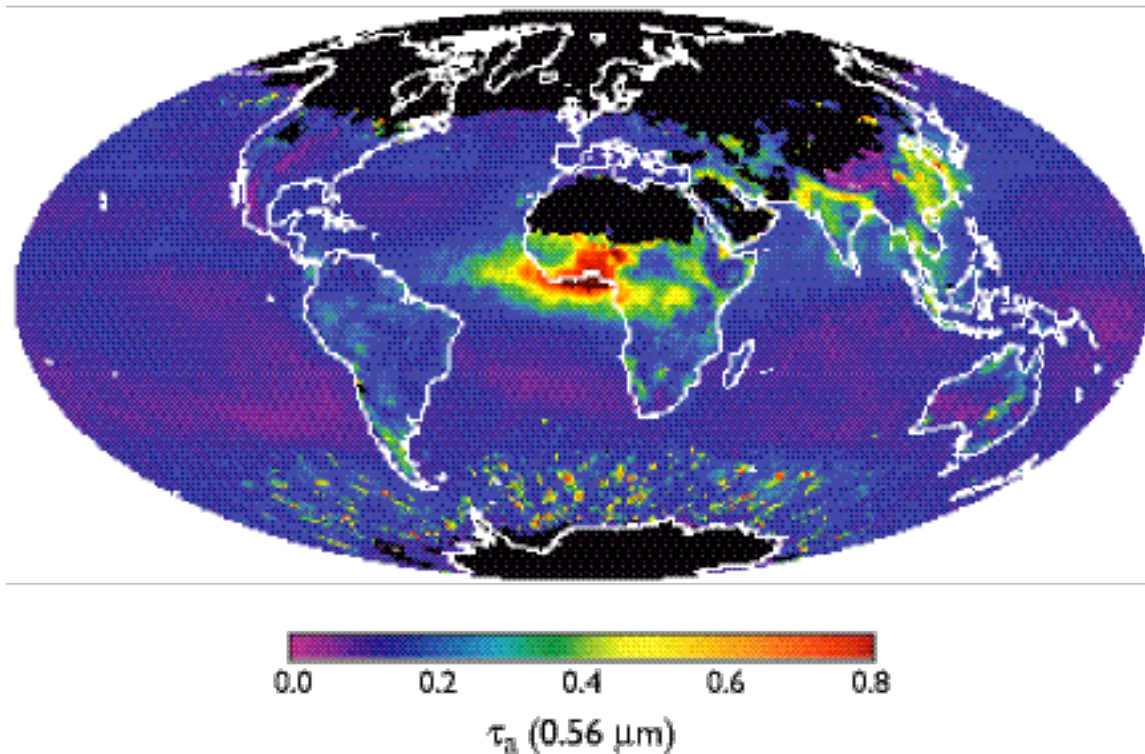


Figure 2. Monthly average aerosol optical thickness at 0.56 μm for January 2002. These data are produced at a $1^\circ \times 1^\circ$ latitude-longitude grid worldwide, and are derived from Terra/MODIS measurements.

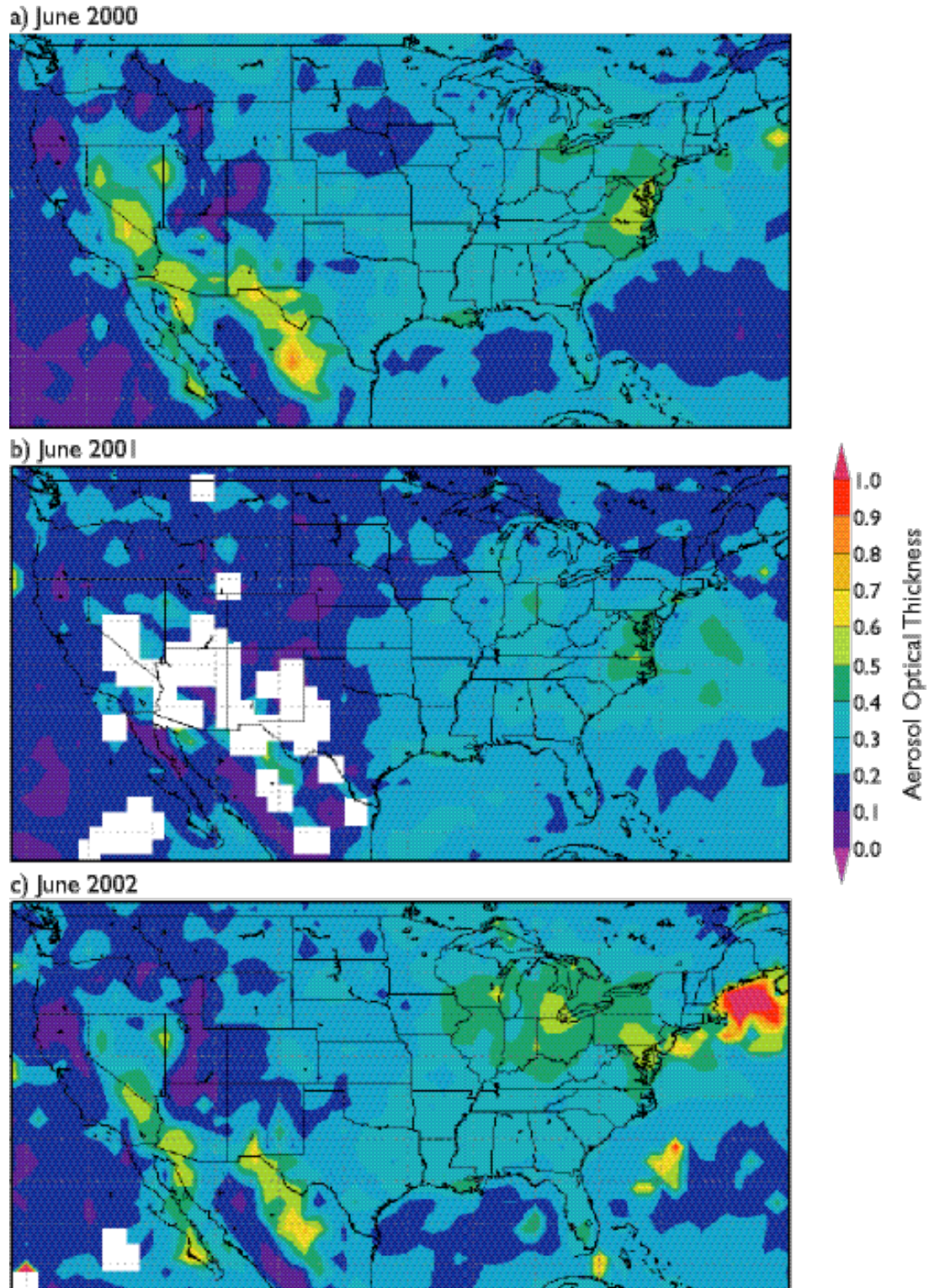


Figure 3: Spatial distribution of aerosol optical thickness for the USA. Observations are from Terra/MODIS for (a) June 2000, (b) June 2001, and (c) June 2002.

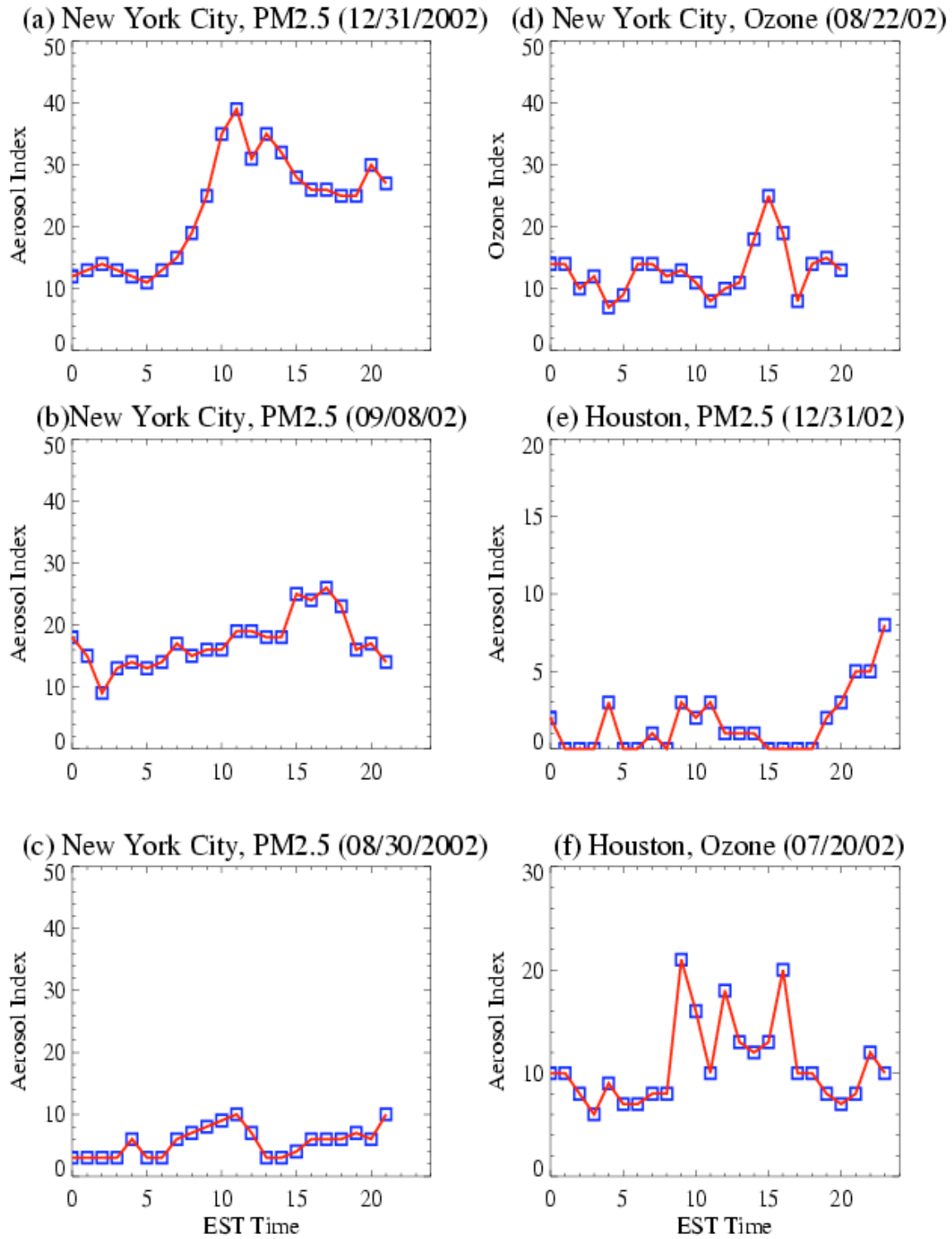


Figure 4: Diurnal variations of urban aerosol for New York and Houston on several days. Data are obtained from EPA PM2.5. Aerosol index is the aerosol quality index. See text for details.

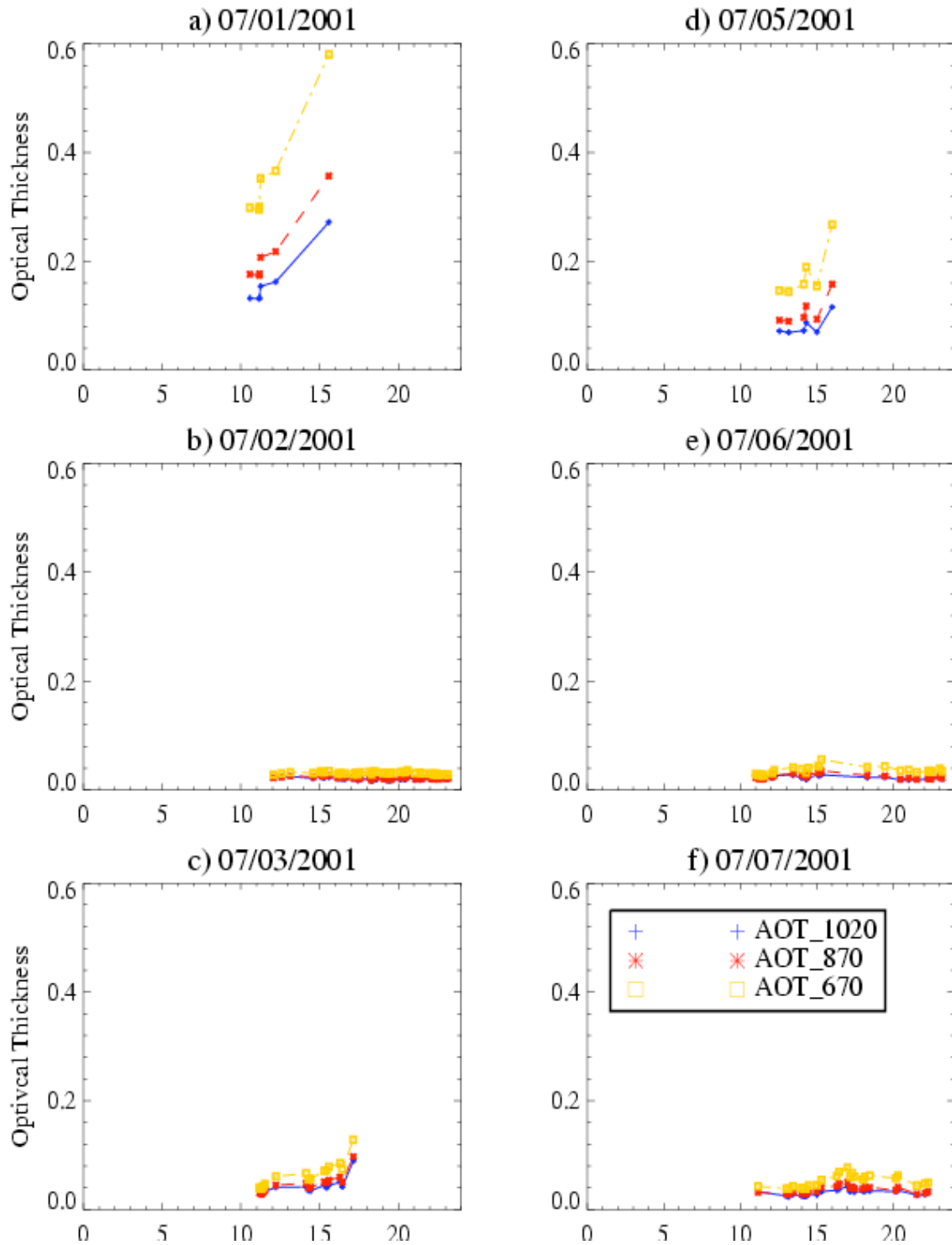


Figure 5. Diurnal variation of aerosol optical thickness for New York at several days of July 2001. Data are based on AERONET GISS station measurements.

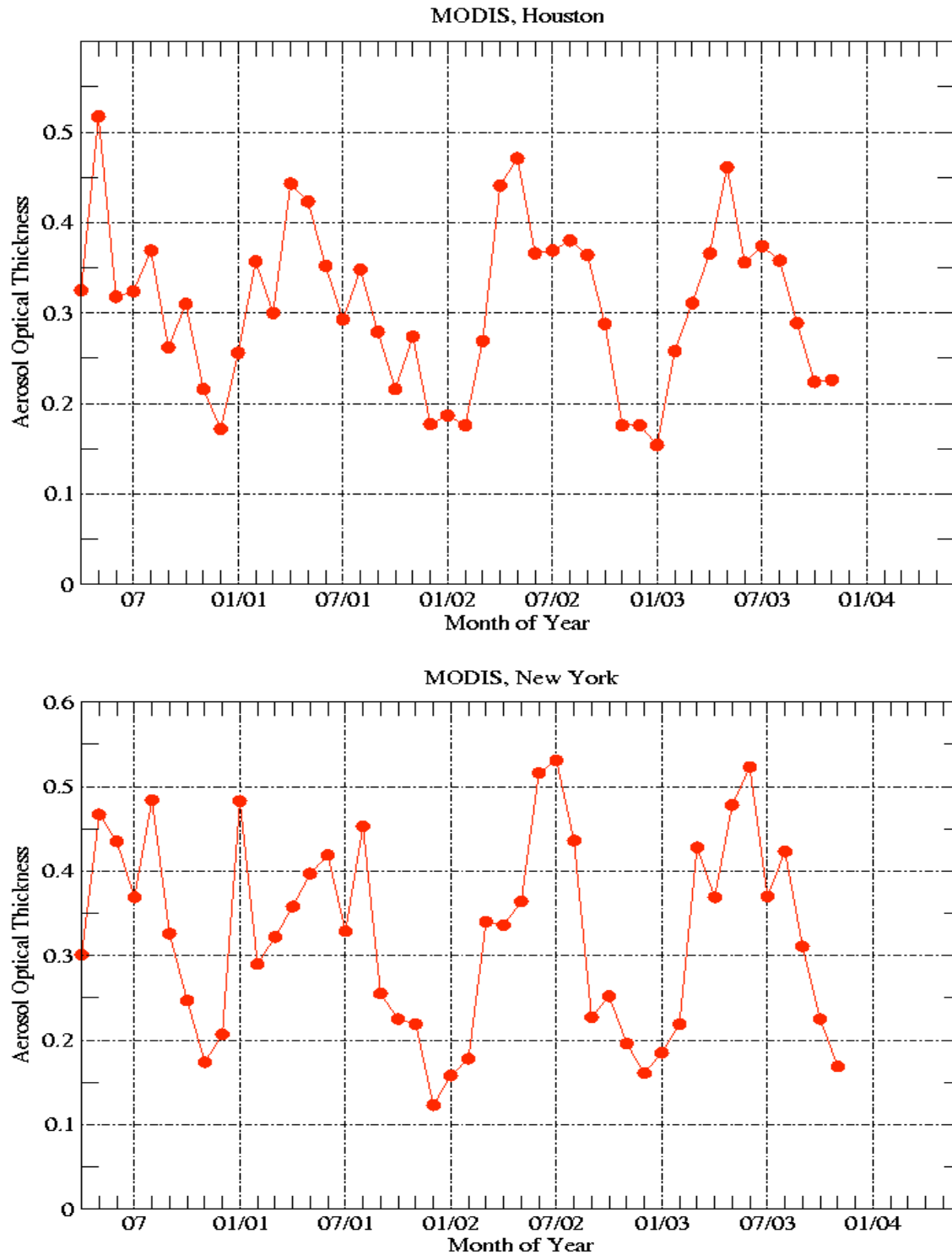


Figure 6. MODIS-derived monthly mean aerosol optical thickness at $0.56 \mu\text{m}$ from April 2000 to September 2003 for (a) Houston and (b) New York City.

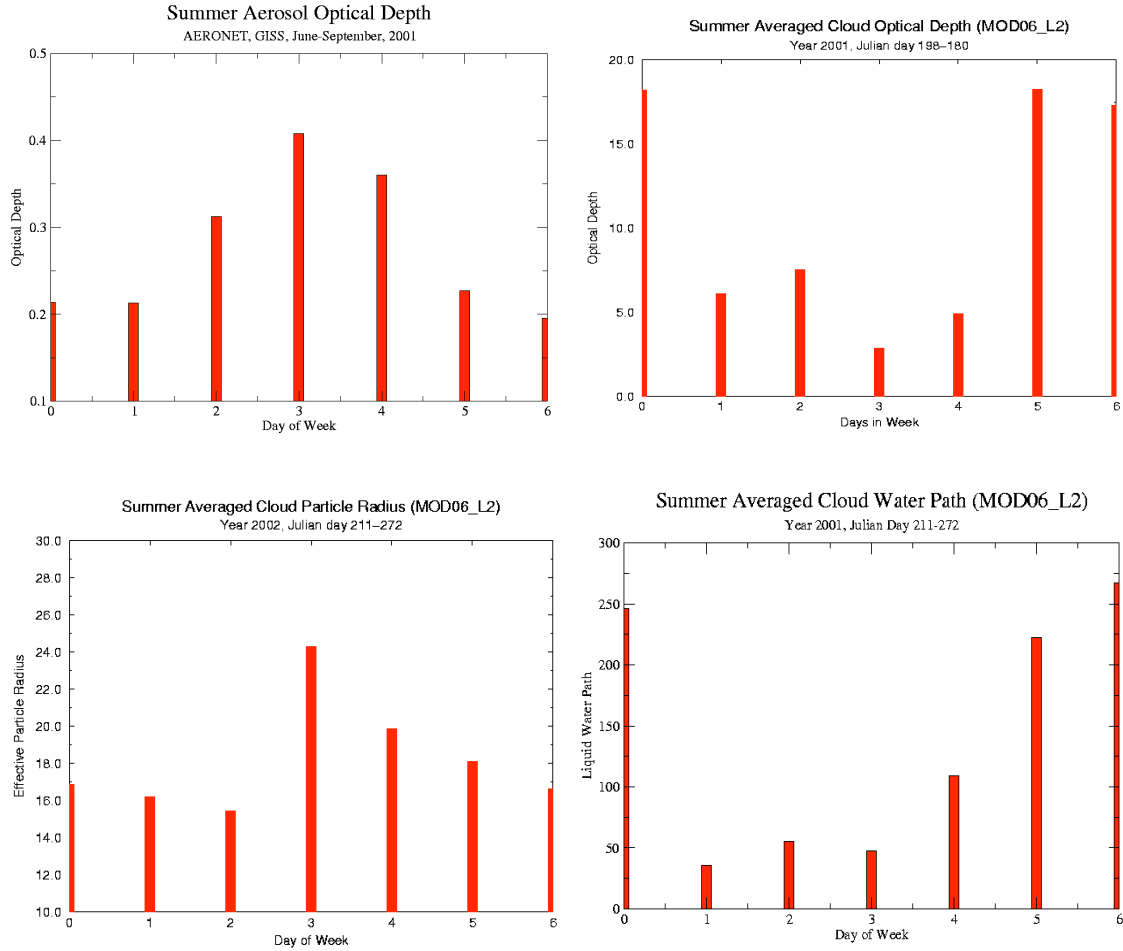


Figure 7. Weekly distribution of (a) the aerosol optical thickness from AERONET at the New York GISS station (41°N , 74°W); (b) the cloud optical thickness at $0.65\ \mu\text{m}$ from the MODIS 1-km resolution level-2 data; (c) cloud effective radius; (d) cloud integrated water path. The data represent the median of the daily averages of June to September 2001 that are then spatially averaged over a $50\ \text{km} \times 50\ \text{km}$ region centered on New York City.

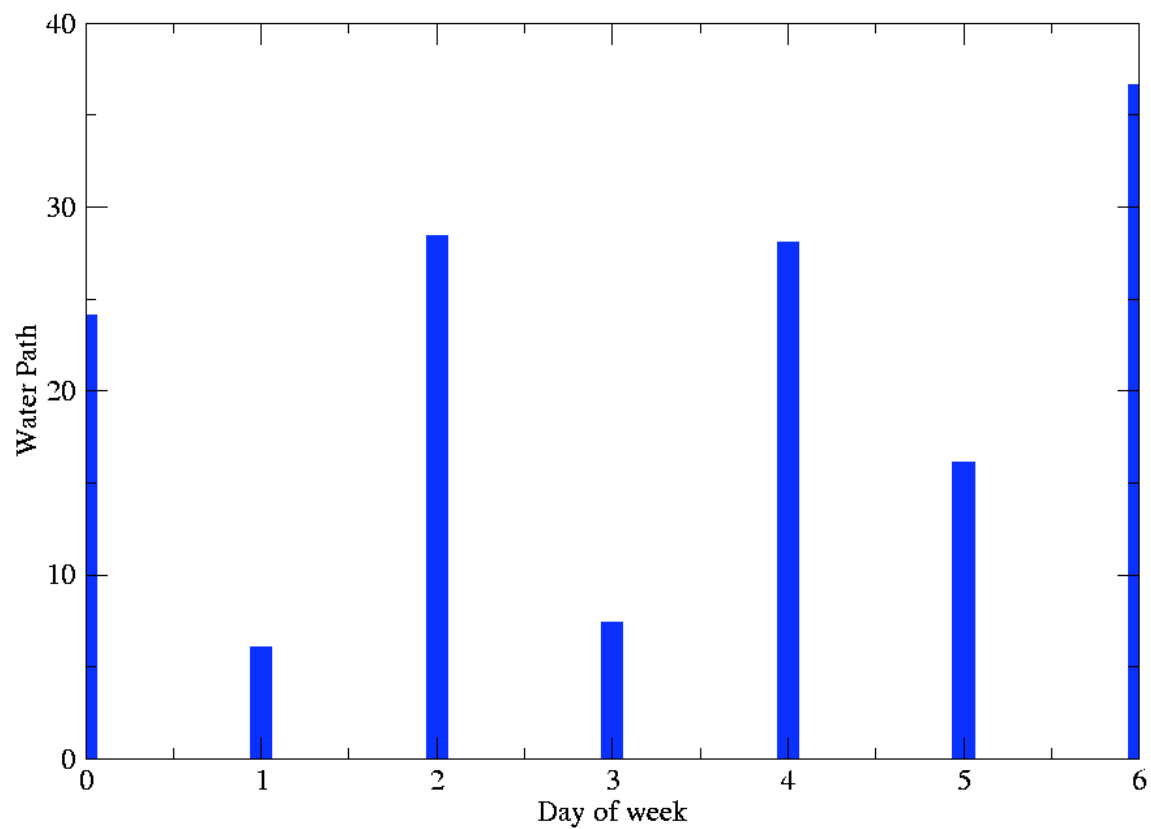


Figure 8. MODIS-derived integrated water path as a function of the day of the week for Houston from July-September 2001.

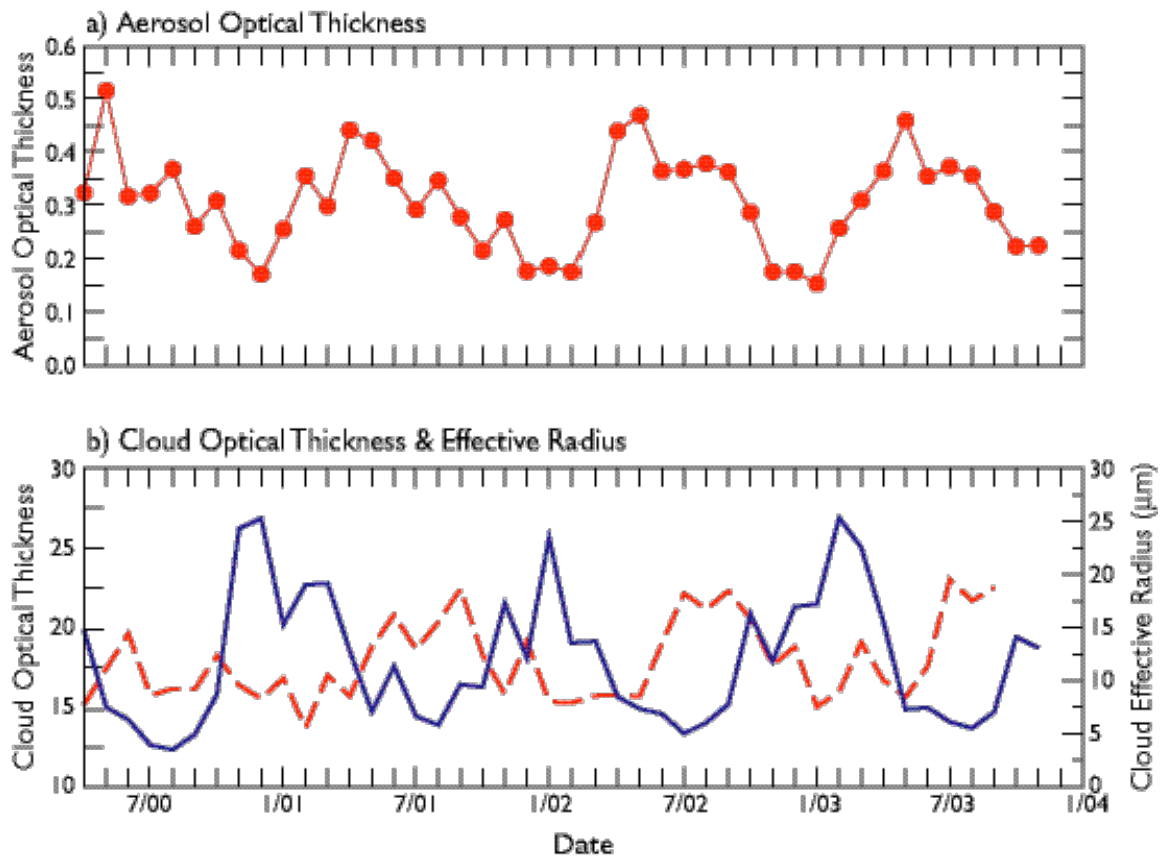


Figure 9. MODIS-derived relationship between (a) aerosol optical thickness and (b) water cloud optical thickness (solid) and effective radius (dashed) for Houston.

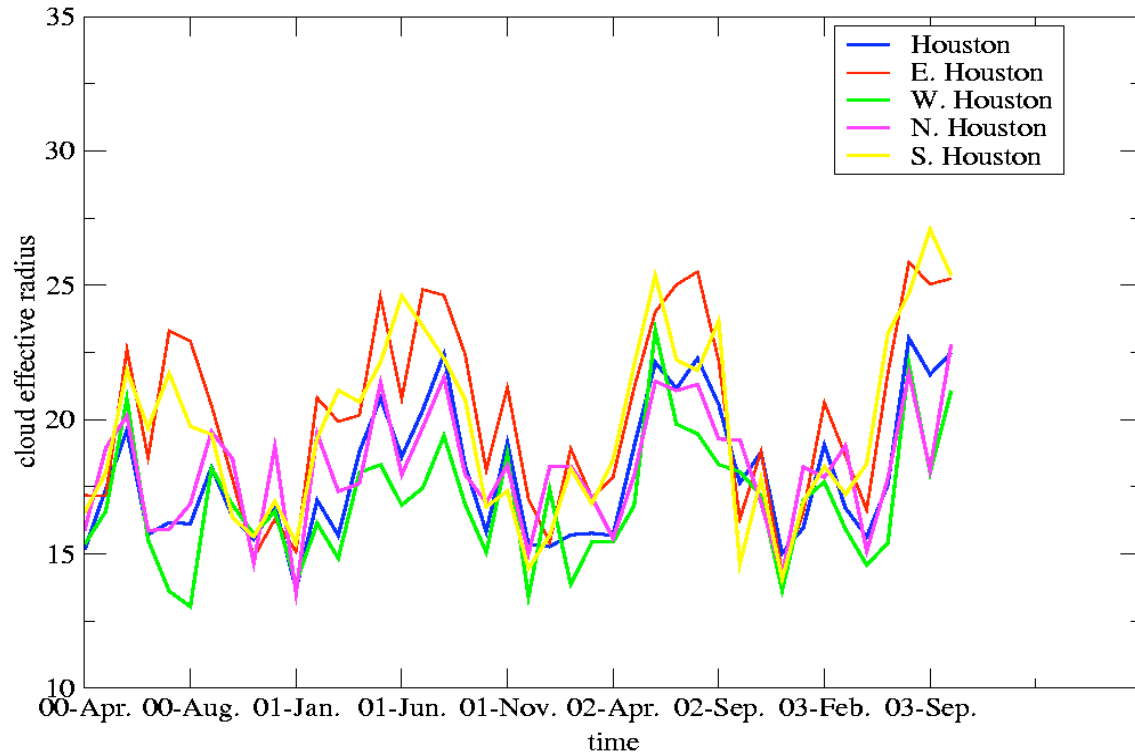


Figure 10. MODIS-derived monthly mean cloud effective radius for Houston, and east, south, north, and south of Houston. Houston is located between 29° and 30°N , and 74° and 75°W .

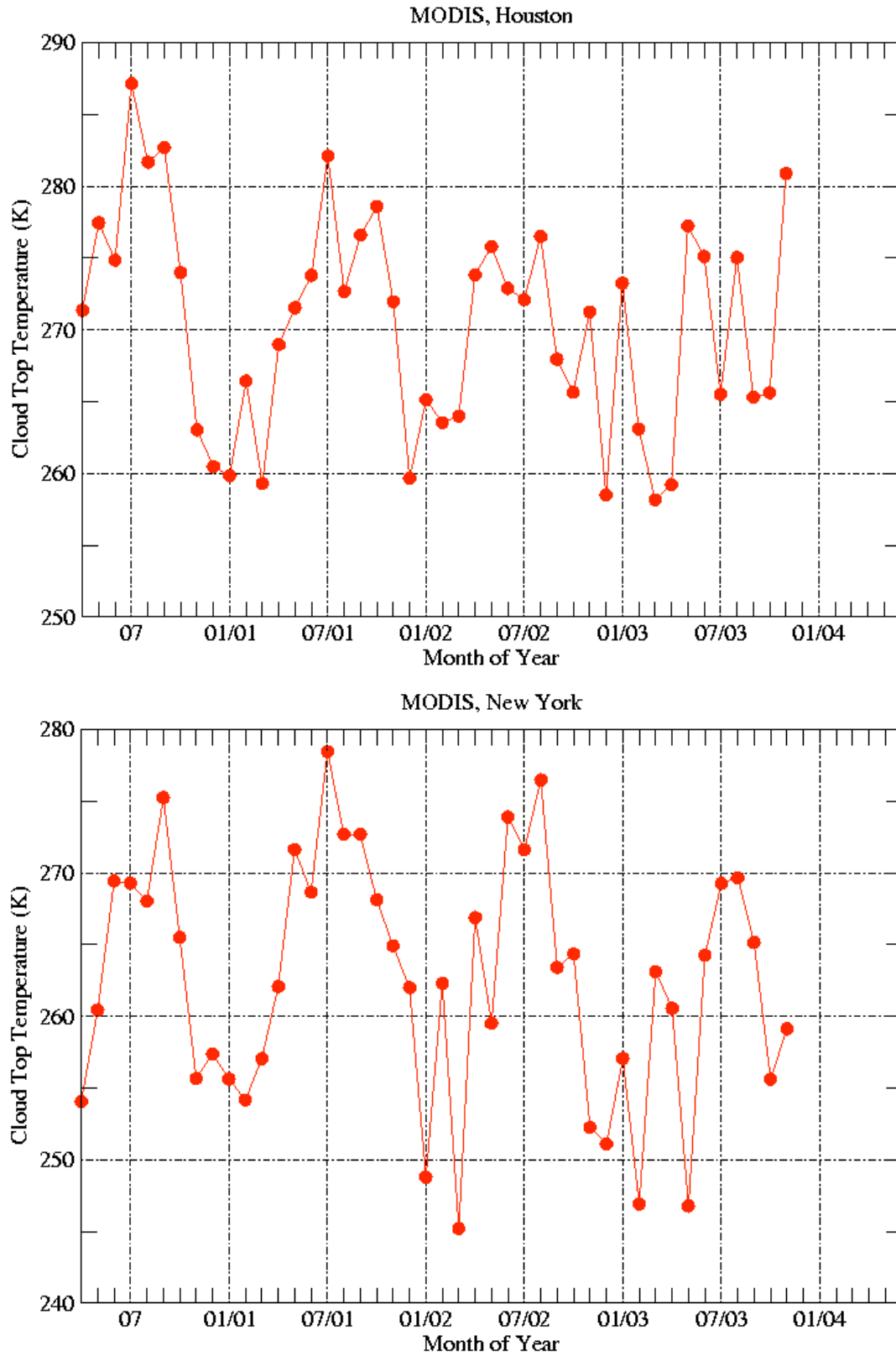


Figure 11. Comparison of cloud top temperature of (a) Houston and (b) New York City derived from Terra/MODIS data.

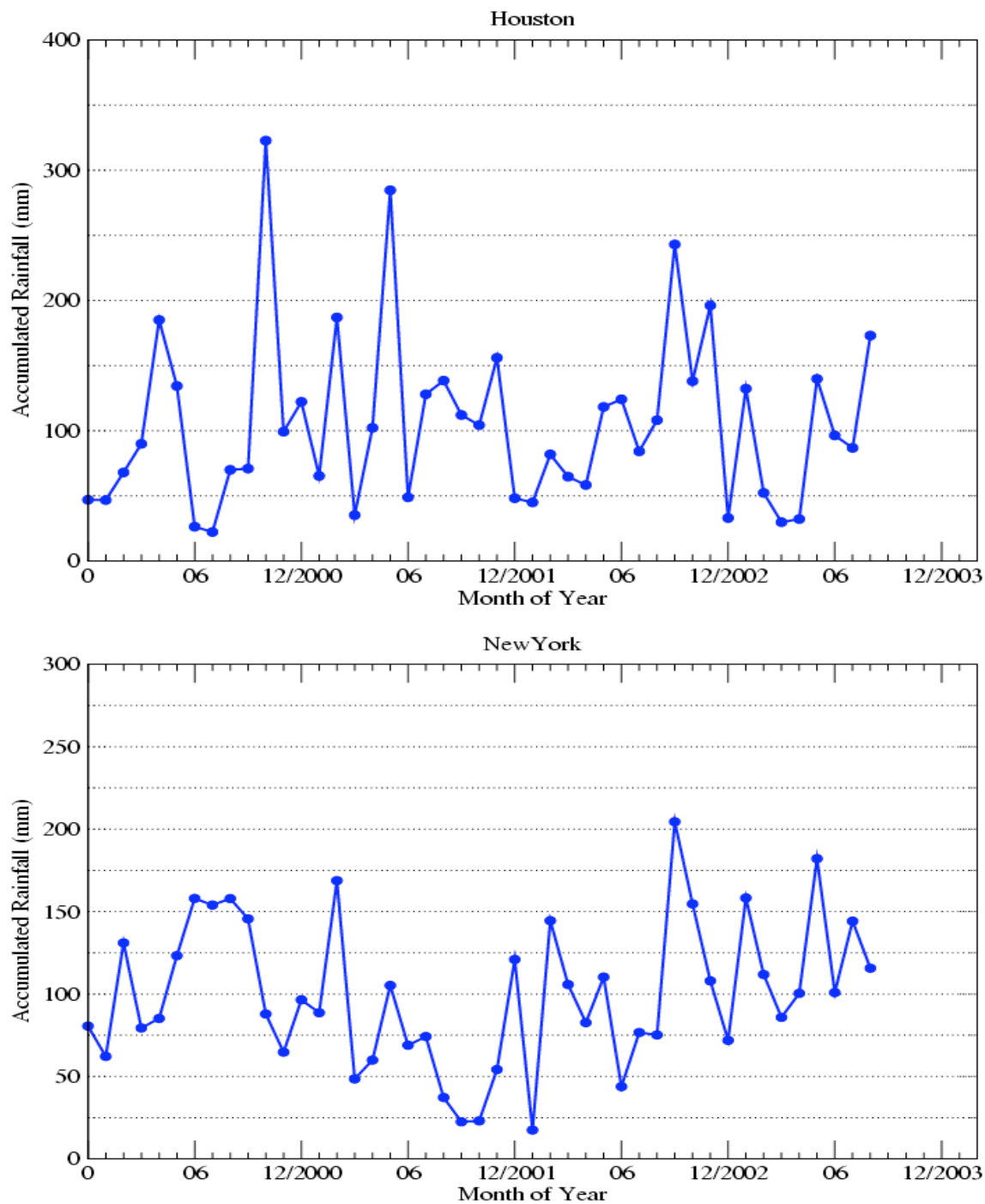


Figure 12. TRMM observed monthly mean rainfall for (a) Houston and (b) New York City from January 2000 to September 2003. The observation product is 3B42, at 1° resolution.

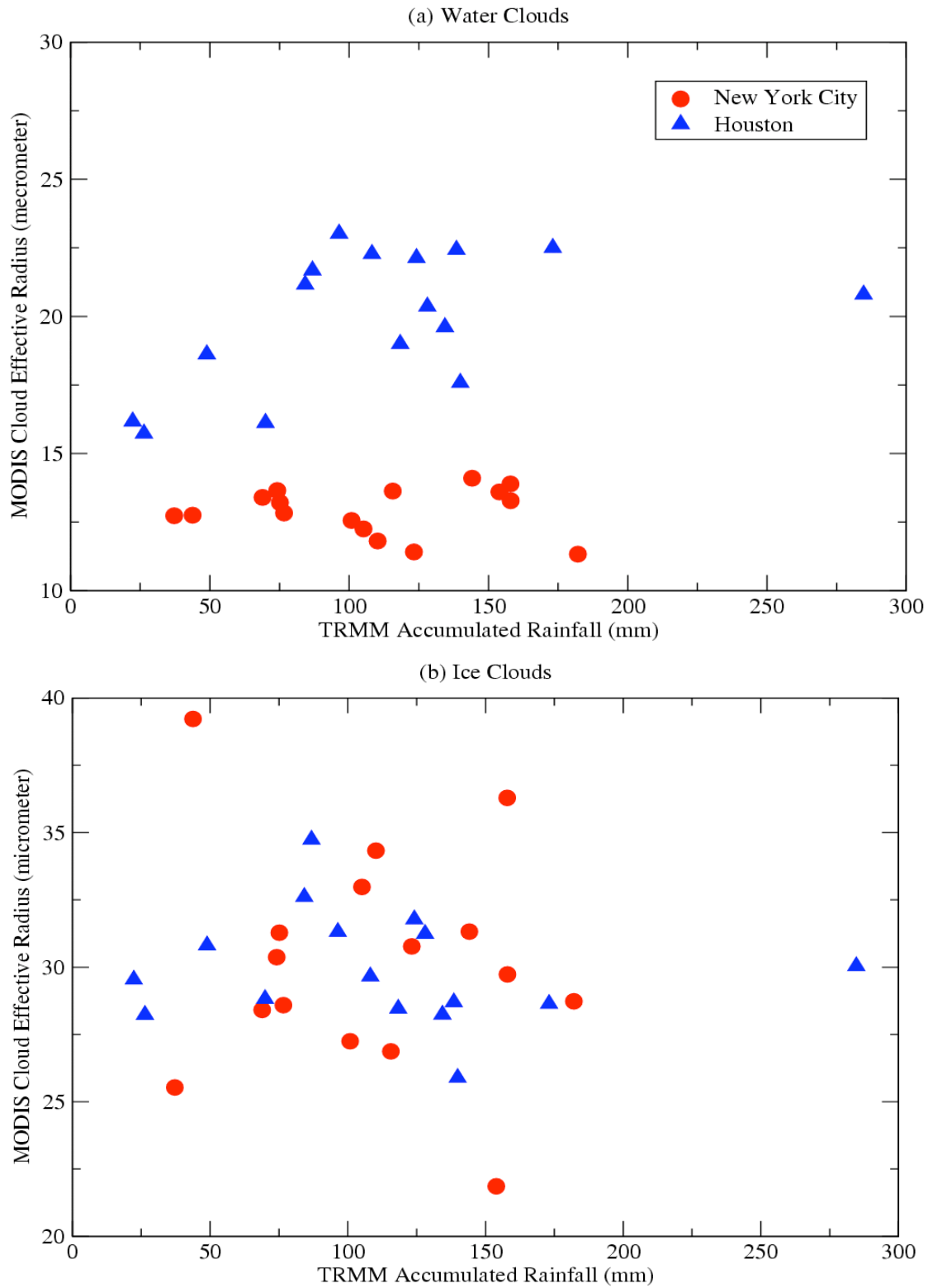


Figure 13. Monthly mean accumulated rainfall vs. cloud effective radius for New York City and Houston (a) for water clouds and (b) for ice clouds.

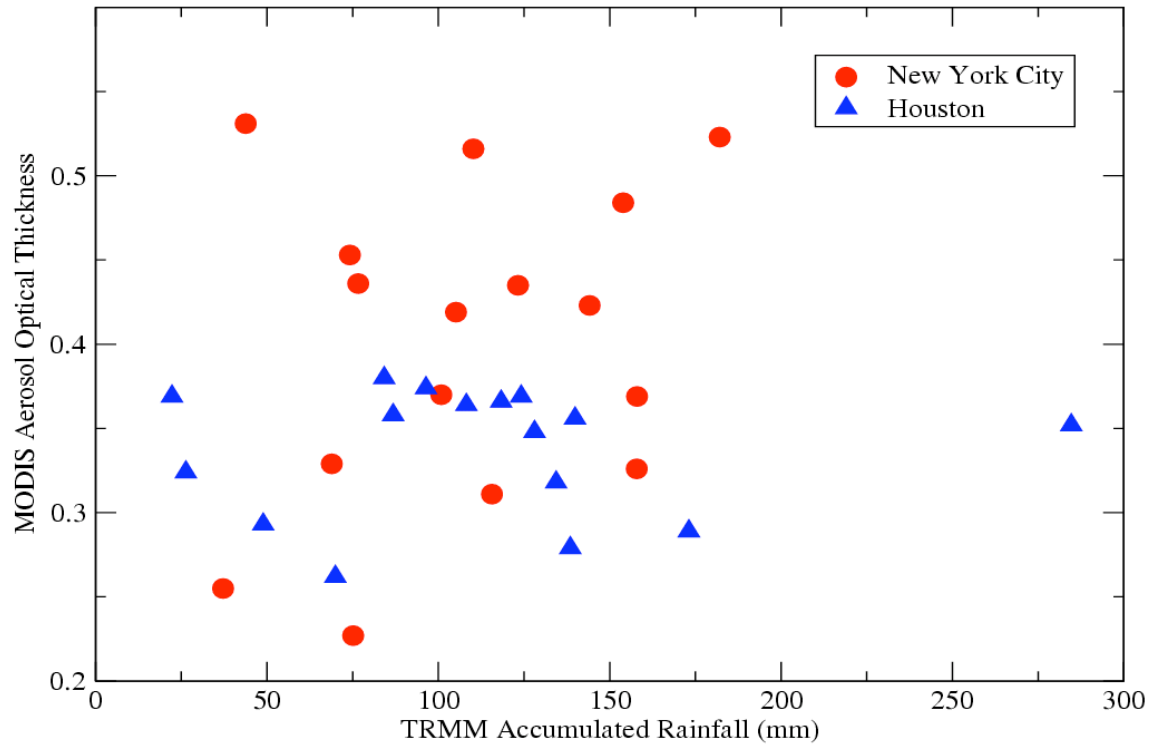


Figure 14. The scatter plot of MODIS aerosol thickness and TRMM-based accumulated rainfall for Houston and New York City, respectively. The data are monthly mean values for the warm season period (June–September) for 2000, 2001, 2002, and 2003.

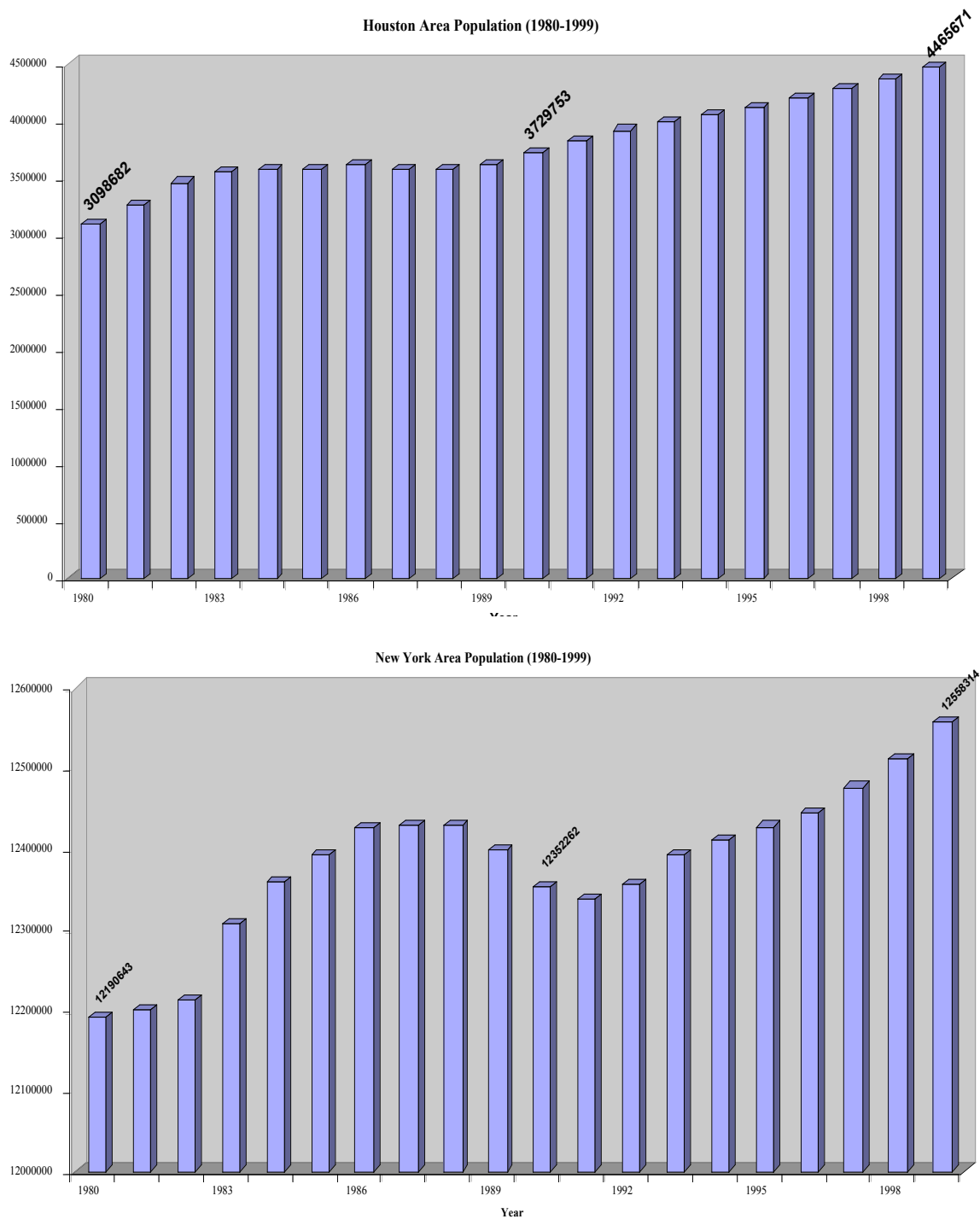


Figure 15. Population density of Houston and New York City metropolitan areas from 1980 – 1999.

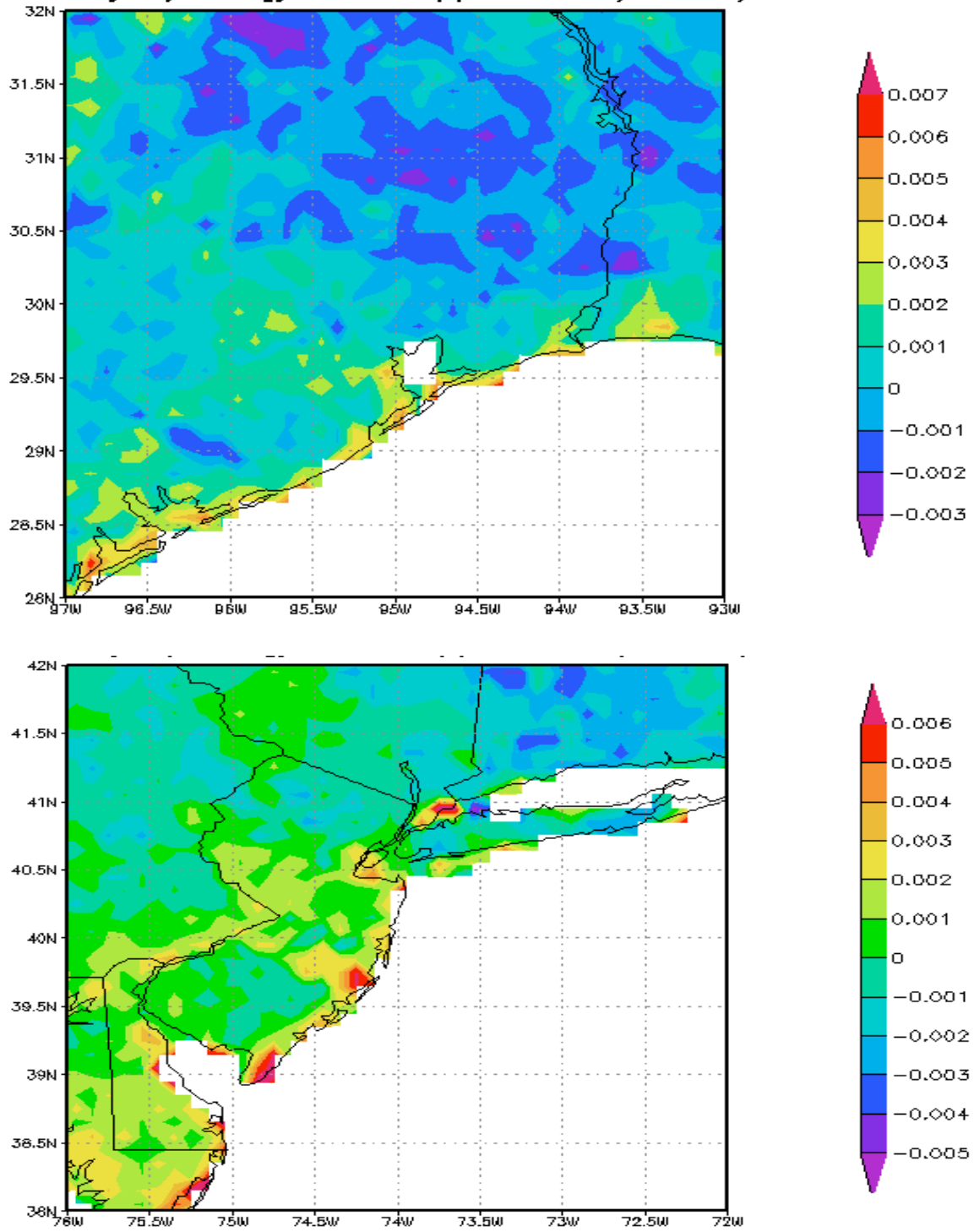


Figure 16. NDVI anomalies from 1981 to 2000 for (a) Houston and (b) New York City.

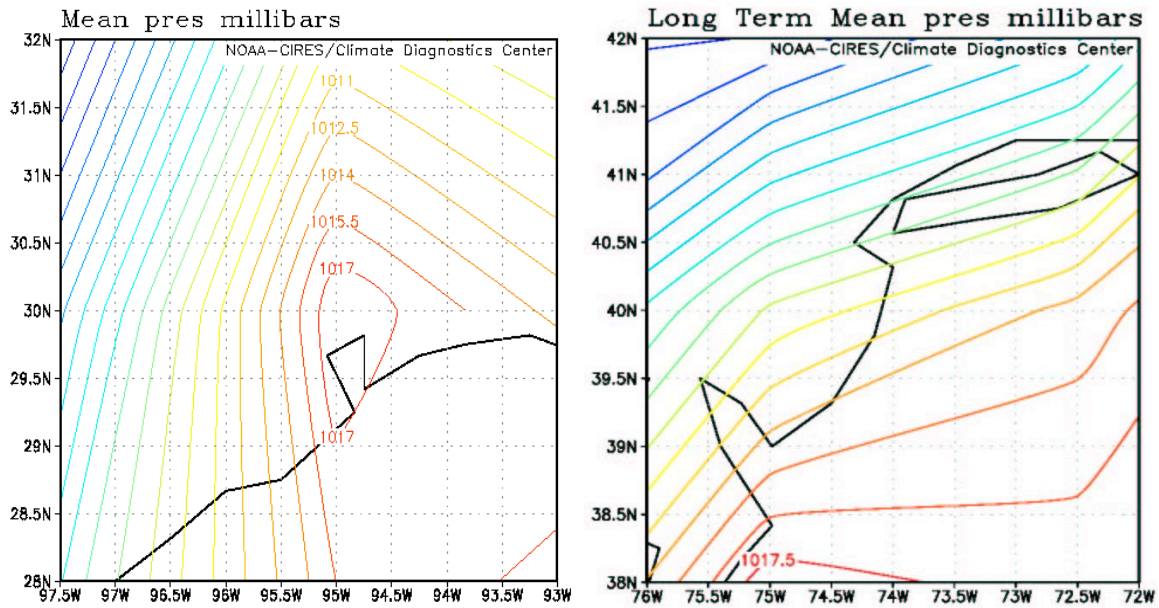


Figure 17. Monthly mean surface pressure for Houston (left) and New York City (right), for July 2000. The data are from NCEP/NCAR reanalysis.